Supplementary Information for

Two-decade surface ozone (O_3) pollution in China: enhanced fine-scale estimations and environmental health implications

Zeyu Yang[1], Zhanqing Li[2*], Fan Cheng[1], Qiancheng Lv[1], Ke Li[3], Tao Zhang[4], Yuyu Zhou[5,6], Bin Zhao[7,8], Wenhao Xue[9], and Jing Wei[2*]

1. Faculty of Geographical Science, Beijing Normal University, Beijing, China
2. Department of Atmospheric and Oceanic Science, Earth System Science Interdisciplinary Center, University of Maryland, College Park, MD, USA
3. Jiangsu Key Laboratory of Atmospheric Environment Monitoring and Pollution Control, Collaborative Innovation Center of Atmospheric Environment and Equipment Technology, School of Environmental Science and Engineering, Nanjing University of Information Science and Technology, Nanjing, China
4. School of Resources and Environment, University of Electronic Science and Technology of China, Chengdu 611731, China
5. Department of Geography, The University of Hong Kong, Hong Kong, China
6. Institute for Climate and Carbon Neutrality, The University of Hong Kong, Hong Kong, China
7. State Key Joint Laboratory of Environmental Simulation and Pollution Control, School of Environment, Tsinghua University, Beijing, 100084, China
8. State Environmental Protection Key Laboratory of Sources and Control of Air Pollution Complex, Beijing 100084, China
9. School of Economics, Qingdao University, Qingdao, China

*Corresponding authors:
zhanqing@umd.edu; weijing@umd.edu

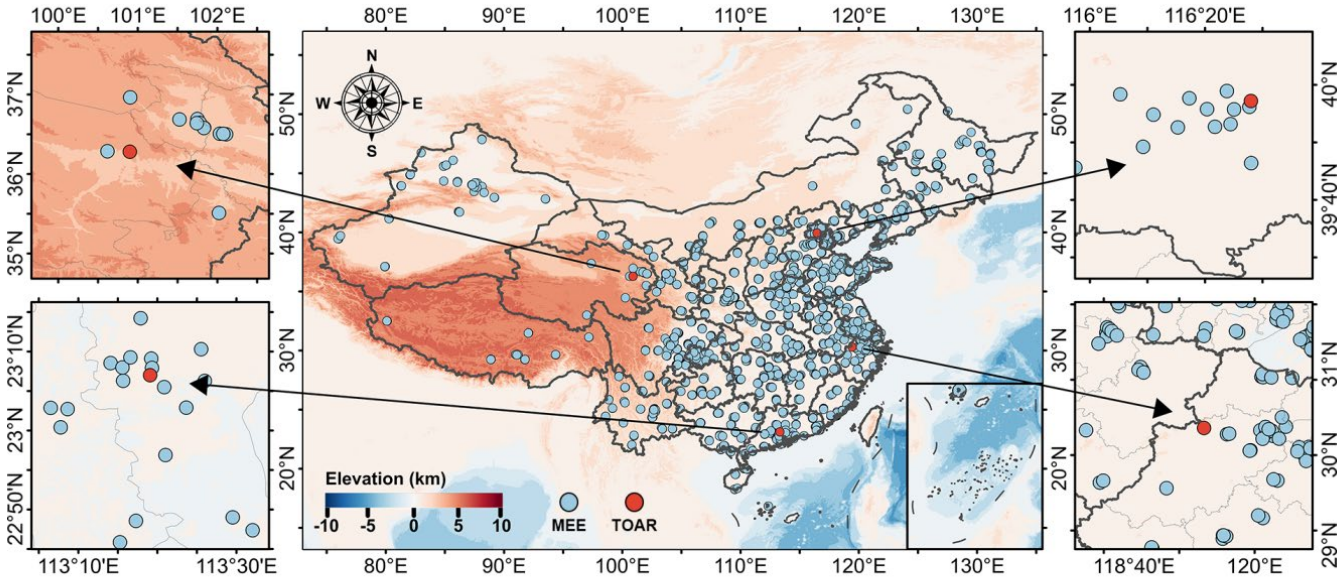

Figure S1. Spatial distributions of ground-based surface O_3 monitoring stations from the Ministry of Ecology and Environment of China (MEE, blue dots) and the Tropospheric Ozone Assessment Report (TOAR, red dots) across China. The black and gray lines on the map indicate provincial and city boundaries, respectively. The background map represents the surface elevation (km).

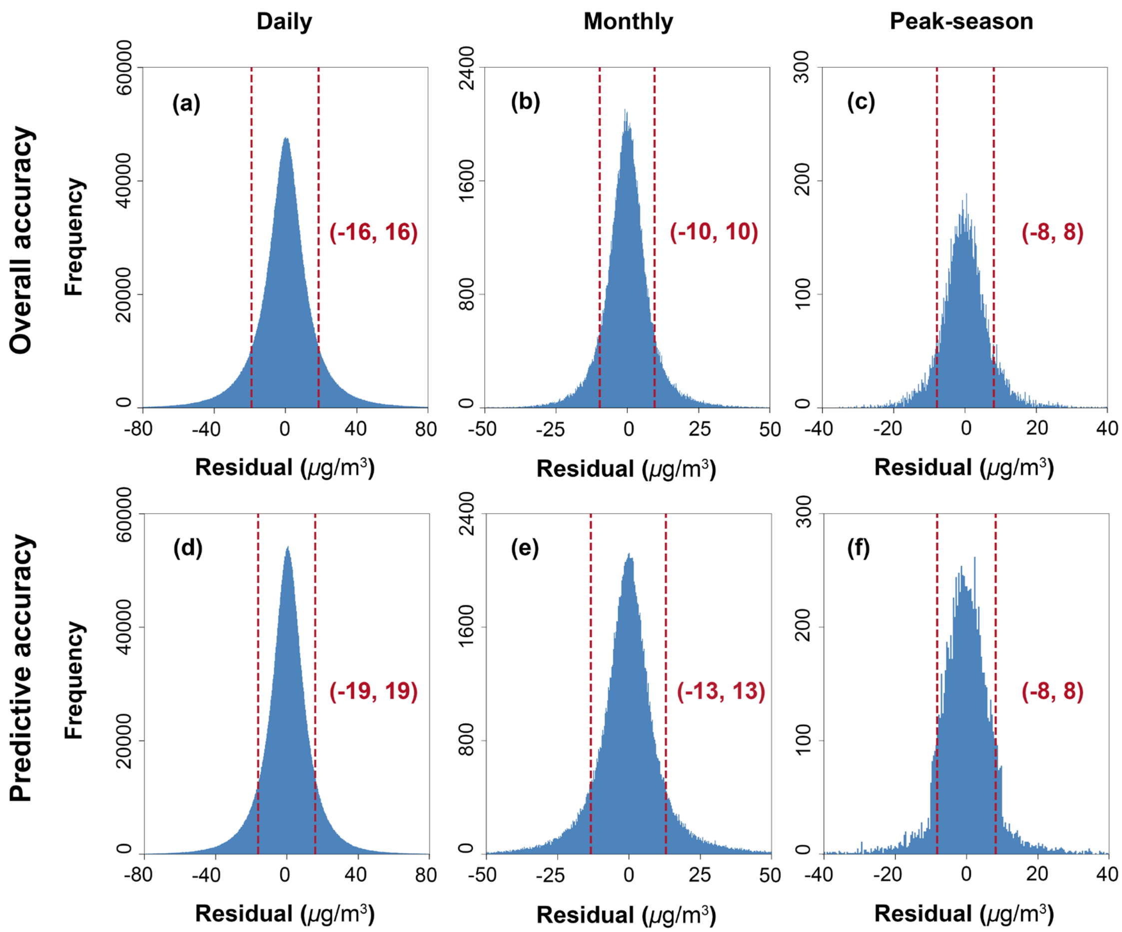

Figure S2. Residual histograms of our MDA8 O_3 (top panels) estimations and (bottom panels) predictions using the out-of-sample and out-of-station cross-validation approaches across daily, monthly, and peak-season scales. The red lines and corresponding numbers represent the range within which 80% of the residuals fall.

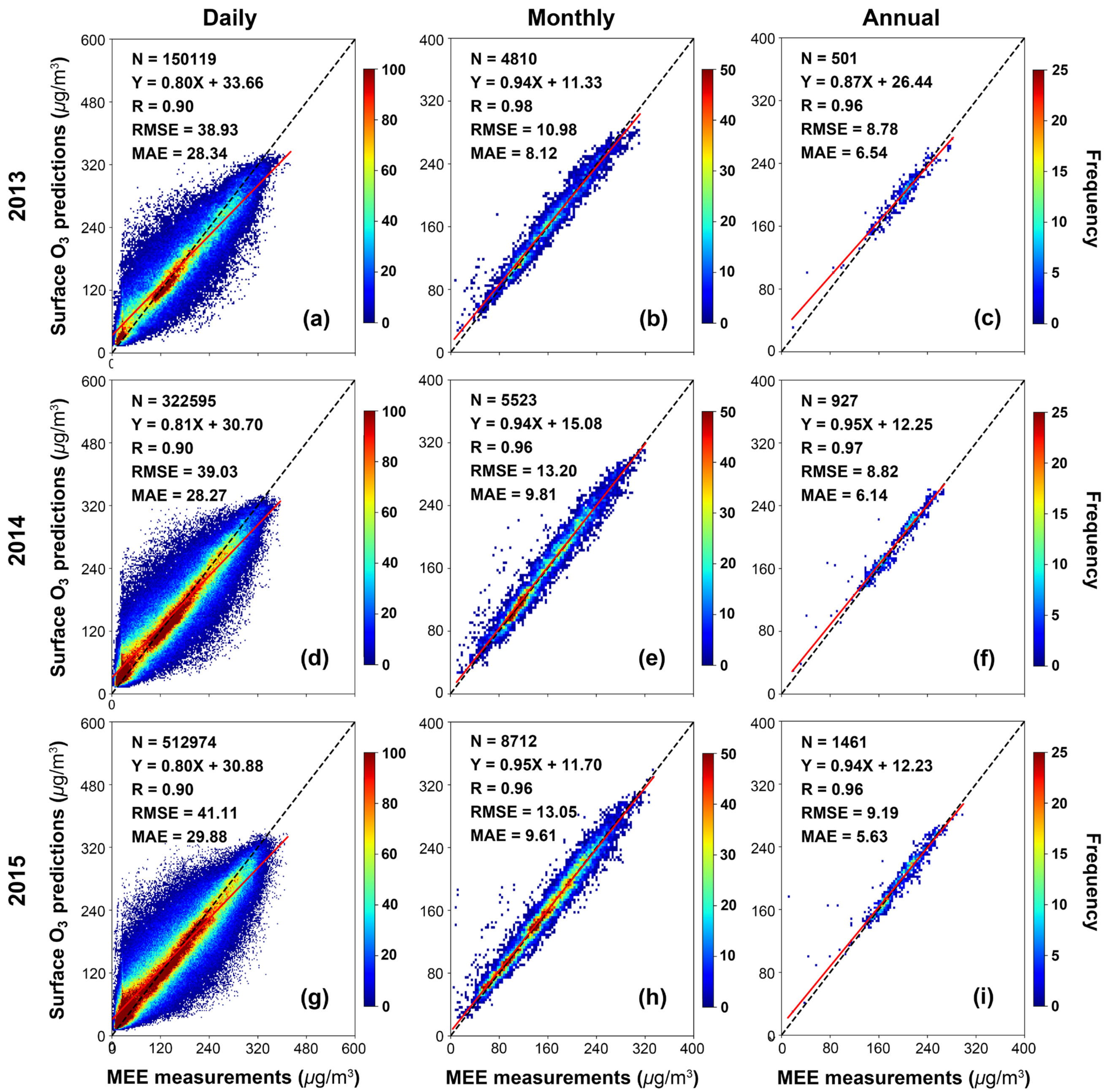

Figure S3. Independent validations between our surface MDA8 O_3 predictions and MEE O_3 measurements for: (a-c) 2013, (d-f) 2014, and (g-i) 2015, from 945, 945, and 1480 monitoring stations, at daily, monthly, and annual levels, respectively.

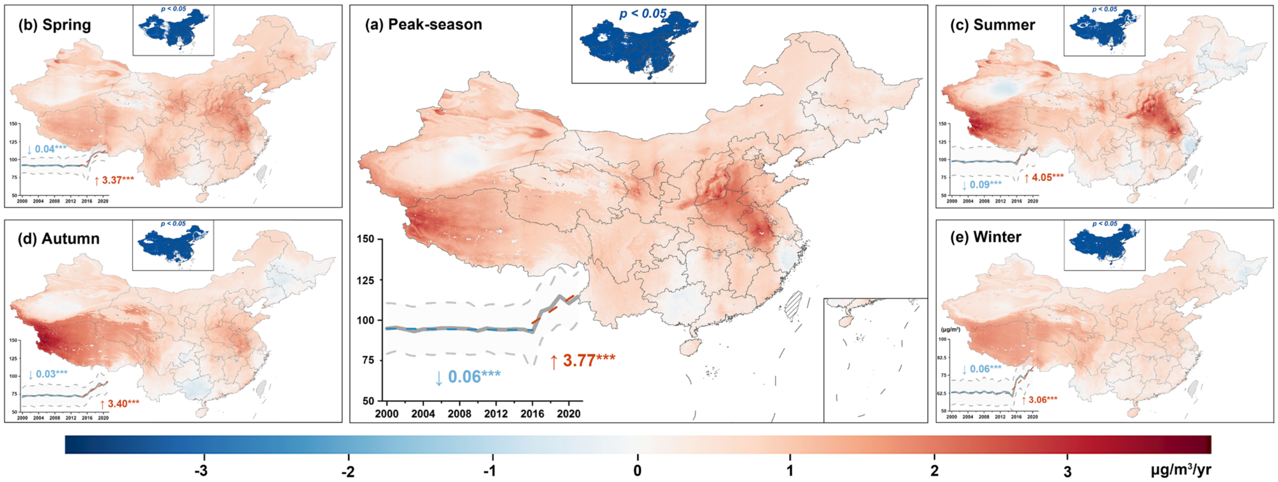

Figure S4. Temporal trends of surface O_3 concentration in mainland China during the 2000–2021 period at (a) peak-season and (b-e) seasonal scales. The maps show seasonal-scale nationwide anomaly variations for (b) spring, (c) summer, (d) autumn, and (e) winter, while panel (a) illustrates the annual peak-season change. The inserted line charts in the lower left corner of each panel show peak-season or seasonal surface O_3 concentrations. The blue (red) dotted line indicates the trend before (after) the breakpoints, with the associated value denoting the trend (*: $p < 0.05$, **: $p < 0.01$, ***: $p < 0.001$).

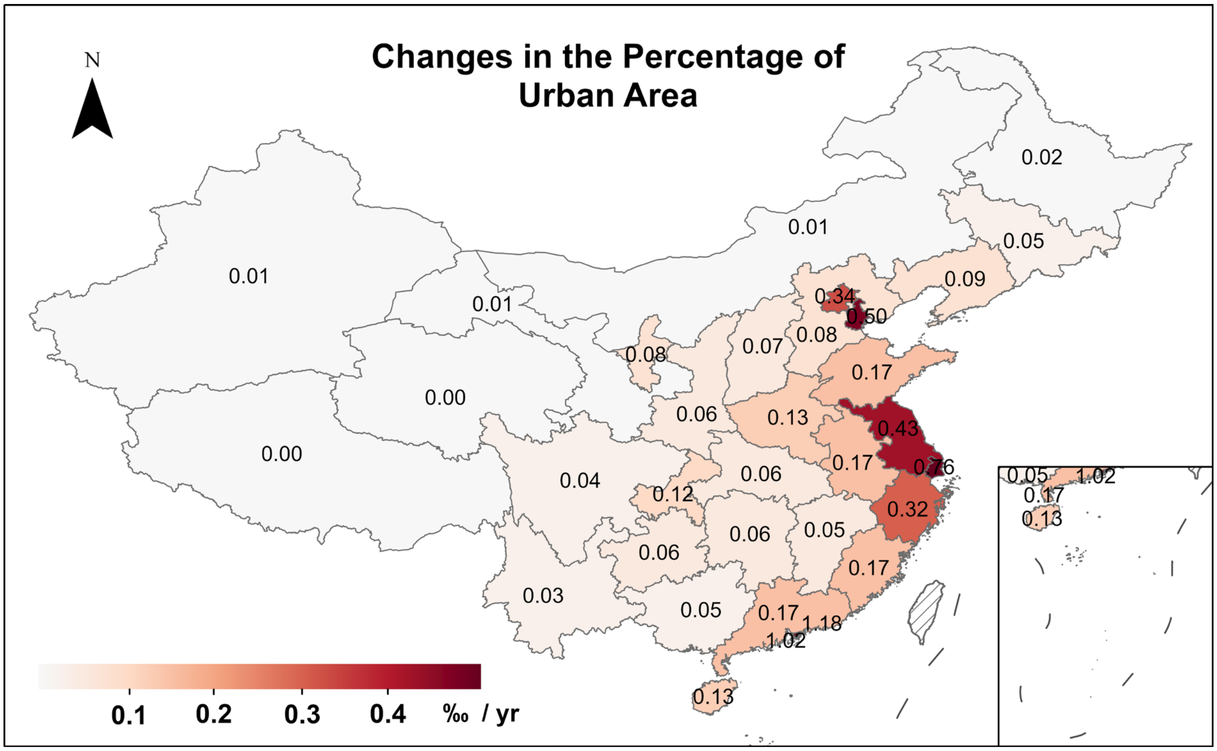

Figure S5. Temporal trends of urban areas for each province in mainland China from 2000 to 2021 using the global annual urban extents dataset (Zhao et al., 2022).

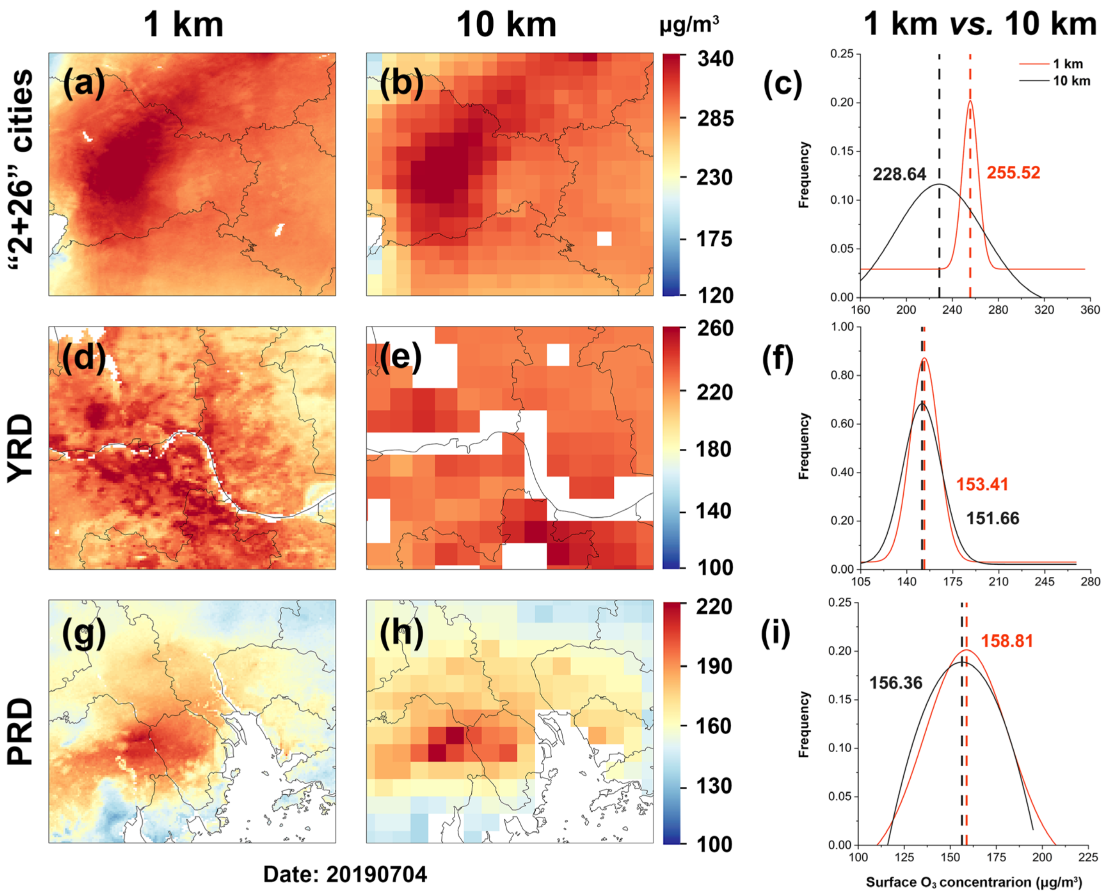

Figure S6. Comparisons of spatial and Gaussian distributions of daily O_3 concentrations at 1-km and 10-km spatial resolutions within the (a-c) "2+26" cities, (d-f) YRD, and (g-i) PRD regions for 4 July 2019. Vertical red (blue) lines represent the peaks of the fitted 1-km (10-km) frequency distributions, with the accompanying numbers representing the peak levels.

Table S1. Overall accuracy and spatial predictive ability of our daily MDA8 O_3 retrievals across major sub-regions in mainland China from 2013 to 2021, using out-of-sample and out-of-station cross-validation approaches.

Region	Overall accuracy			Spatial predictive ability		
	R^2	RMSE (μg/m^3)	MAE (μg/m^3)	R^2	RMSE (μg/m^3)	MAE (μg/m^3)
BTH	0.92	16.64	10.56	0.89	19.51	12.22
YRD	0.87	17.84	11.95	0.83	20.50	13.35
SCB	0.88	16.63	11.45	0.85	19.19	13.01
PRD	0.87	18.37	12.44	0.84	20.94	14.20
TP	0.85	11.86	8.09	0.62	19.08	13.28
China	0.89	15.77	10.48	0.84	18.74	12.36

BTH: Beijing-Tianjin-Hebei, YRD: Yangtze River Delta, SCB: Sichuan Basin, PRD: Pearl River Delta, TP: Tibetan Plateau.

Table S2. Comparison of previous long-term (more than 5 years) studies estimating O_3 concentrations for the entirety of mainland China.

Temporal resolution	Temporal coverage	Spatial resolution	Gapless	Model	CV-R^2	RMSE ($\mu g/m^3$)	Reference
Daily	2013-2020	0.1° × 0.1°	Yes	data-fusion	0.70	26.00	Xue et al., 2020
Daily	2005-2017	0.1° × 0.1°	No	XGBoost	0.76	21.47	Liu et al., 2020
Daily	2013-2020	0.1° × 0.1°	Yes	STET	0.87	17.10	Wei et al., 2022a
Daily	2016-2020	0.1° × 0.1°	Yes	3D-CNN	0.88	15.65	Mu et al., 2023
Monthly	2005-2019	0.05° × 0.05°	Yes	RF	0.87	13.03	Zhu et al., 2022
Daily	2013-2017	0.05° × 0.05°	Yes	NAQPMS	0.89	14.1	Wang et al., 2020
Daily	2015-2021	0.05° × 0.05°	Yes	DF	0.91	12.47	Chen et al., 2023
Daily	**2013–2021**	**0.01° × 0.01°**	**Yes**	**4D-STDF**	**0.89**	**15.77**	**Our study**

STET: Space-Time Extra-Trees; 3D-CNN: Three-Dimensional Convolutional Neural Network; RF: Random Forest; NAQPMS: Nested Air Quality Prediction Modeling System; DF: Deep Forest

Reference:

Chen, B., Wang, Y., Huang, J., Zhao, L., Chen, R., Song, Z., & Hu, J., 2023. Estimation of near-surface ozone concentration and analysis of main weather situation in China based on machine learning model and Himawari-8 TOAR data. Sci. Total Environ., 864, 160928. https://doi.org/10.1016/j.scitotenv.2022.160928

Liu, R., Ma, Z., Liu, Y., Shao, Y., Zhao, W., & Bi, J., 2020. Spatiotemporal distributions of surface ozone levels in China from 2005 to 2017: A machine learning approach. Environ. Int., 142, 105823. https://doi.org/10.1016/j.envint.2020.105823

Mu, X., Wang, S., Jiang, P., Wang, B., Wu, Y., & Zhu, L., 2023. Full-coverage spatiotemporal estimation of surface ozone over China based on a high-efficiency deep learning model. Int J. Appl Earth Obs, 118, 103284. https://doi.org/10.1016/j.jag.2023.103284

Wang, Y., Wild, O., Chen, X., Wu, Q., Gao, M., Chen, H., Qi, Y., & Wang, Z., 2020. Health impacts of long-term ozone exposure in China over 2013−2017. Environ. Int., 144, 106030. https://doi.org/10.1016/j.envint.2020.106030

Wei, J., Li, Z., Li, K., Dickerson, R.R., Pinker, R.T., Wang, J., Liu, X., Sun, L., Xue, W., & Cribb, M., 2022a. Full-coverage mapping and spatiotemporal variations of ground-level ozone (O_3) pollution from 2013 to 2020 across China. Remote Sens. Environ., 270, 112775. https://doi.org/10.1016/j.rse.2021.112775

Xue, T., Zheng, Y., Geng, G., Xiao, Q., Meng, X., Wang, M., Li, X., Wu, N., Zhang, Q., & Zhu, T., 2020. Estimating Spatiotemporal Variation in Ambient Ozone Exposure during 2013−2017 Using a Data-Fusion Model. Environ. Sci. Technol., 54, 14877-14888. 10.1021/acs.est.0c03098

Zhao, M., Cheng, C., Zhou, Y., Li, X., Shen, S., & Song, C., 2022. A global dataset of annual urban extents (1992–2020) from harmonized nighttime lights. *Earth Syst. Sci. Data*, 14, 517–534. https://doi.org/10.5194/essd-14-517-2022

Zhu, Q., Bi, J., Liu, X., Li, S., Wang, W., Zhao, Y., & Liu, Y., 2022. Satellite-Based Long-Term Spatiotemporal Patterns of Surface Ozone Concentrations in China: 2005−2019. Environ. Health Persp., 130, 27004. 10.1289/EHP9406